

Low Emission Combustion

By
Kyle Gompertz

A report submitted to the affiliates of
the University Turbine Systems Research Program
in partial fulfillment of the UTSR Fellowship

Combustor Augmenter Nozzle Module Center
Pratt & Whitney
September 15, 2008

Acknowledgements

I would like to acknowledge some of the people that made this wonderful learning experience possible. I am grateful to Misty Edwards, Dick Tuthill, Urmila Reddy, Tim Snyder, Al Veninger, Christine Blanchard, Jeff Melman, Craig Smith, Barry Schlein, and my advisor, Dr. Jeffrey Bons. Thank you to all for kindness, teaching me, and being excellent examples to follow. It has been my privilege and a pleasure to participate in this program.

Abstract

An existing Fortran code was used to construct secondary flow models in order to assess the total pressure loss and outflow margins for two combustors. Each component model is comprised of a series of chambers interconnected by various types of resistors to the gas path. The flow code solves the unknown chamber pressure and flow rates through successive iterations until the flow rates are balanced. One of the combustors for which a model was devised is a lower emission industrial version of a conventional diffusion combustor can which has recently been the subject of engine testing. The secondary flow model of this combustor can was used to aid in the analysis of engine test results and in revisions for the next iteration of the design. In addition to pressure loss calculation, comparisons were made between thermal paint data, embedded thermocouple measurements, temperature crystal measurements, and pre-test thermal predictions. The analysis served to validate the thermal model and assist structural analysis of engine results. Another flow model was constructed for a new concept combustor employing regenerative cooling. The design is in the early stages of development. Significant contributions to guide the design were made by surveying competitor designs with similar requirements.

Introduction to Low Emission Combustor Design

From the most modern technology to retrofits of older machines, emission requirements for gas turbine power plants have become more stringent during the past 10 years. Environmental agencies around the world are now requiring ever lower rates of emission of NO_x and other pollutants from both new and existing gas turbines.

The significant products of combustion in gas turbine engines are oxides of nitrogen (NO and NO_2 ; collectively called NO_x), oxides of Sulfur (SO SO_2 ; SO_x), unburned hydrocarbons (UHCs), CO and CO_2 . Aside from fuel-bound Nitrogen and prompt NO_x , a chemical reaction sequence known as the Zeldovich mechanism is responsible for NO_x formation. The mechanism is well known and states that NO_x formation is principally an exponential function of temperature, and a linear function of the time for which the hot gases are at flame temperature. Flame temperature is a unique function of equivalence ratio. The maximum temperature is attained at the stoichiometric equivalence ratio, and minimal flame temperature on the *lean* end of the spectrum.

The design challenges associated with very lean combustion involve ensuring ignition and flame stability without blowouts, flashback or flame fluctuations. These challenges are driven by the need to operate the combustor at low flame temperatures to achieve very low NO_x emissions.

Emissions Control Methods

There are three principal methods for controlling gas turbine emissions:

- 1) Injection of a diluents such as water or steam into the burning zone of a conventional (diffusion flame) combustor
- 2) Design of the combustor to limit the formation of pollutants in the burning zone by utilizing “lean-premixed” combustion technology, which includes both DLN combustors and catalytic combustors.
- 3) Catalytic clean-up of NO_x and CO from the gas turbine exhaust (usually used in conjunction with the other two methods)

Combustor 1

Combustor 1 is an aero derivative adapted for industrial application. It is operated at >90% power in tandem with a power turbine. Water is used to lower the flame temperature and suppress the formation of NO_x. Water addition is critical in the balance of NO_x and CO. CO emissions increase as the flame temperature decreases because a high temperature is required to oxidize CO to CO₂. The baseline combustor design is film cooled with louvers which lay a film down on the hot side surface. This film of cooler air quenches the CO and prevents the oxidation to CO₂. Combustor 1 has been guaranteed at 60 ppm of CO.

Secondary Flow Model

The secondary flow model focuses only on the liner cooling flow. The total pressure profile is determined by performing a pressure balance throughout the coolant passage on the cold-side of the liner which includes impingement, dilution grommet blockage and cooling exit holes. Engine data is used to specify inlet and exit boundary.

Combustor 1 was recently subjected to engine testing has two types of coolant inlet orifices. It has an annular feed a row of impingement cooling holes at the inlet. Ultimately, the two inlet paths were modeled as one lumped inlet due to the difficulty modeling the interaction of the two streams. The impingement cooling jet in cross flow creates a blockage for the fluid entering through the ram feed inlet and the ram feed in turn causes the impingement jets to bend over. The mass flow measured in cold flow tests was matched with the model output to determine the lumped discharge coefficient of the physical area. The data matching results are summarized in Table 1, and the resulting lumped discharge coefficient used is 0.3629.

Table 1. Cold flow data matching summary

Lumped Inlet Cd	FABL Computed Mass Flow (pps)	Cold Flow: Measured Nozzle Mass Flow (pps)	dP/P	P _{Us} (psia)	P _{Ds} (psia)	T _{amb} (°F)
0.3587	0.1314	0.13135	2.07%	14.4255548	14.1274807	71.8486988
0.3685	0.163	0.16297	3.10%	14.4255548	13.9778498	71.8486988
0.3615	0.1841	0.18413	4.08%	14.4255548	13.8363254	71.8486988
0.3629	Average					

The low lumped discharge coefficient may be explained by the fact that the measured value captures the effects of blockages neglected in the model.

The flow restriction, losses and wake blockage of the combustion grommets were neglected since each has an impingement jets just downstream. The dilution grommets (of different sizes) were modeled with compressible flow loss resistor with essentially 3 steps:

1. contraction from upstream area to throat; no total pressure loss
2. imposed K-loss = 0.15 downstream of minimum cross-section area
3. wake extended 2 grommet diameters downstream of throat to account for wake blockage

The K-loss coefficient represents the total pressure change as a kinetic energy penalty and is given by Eqn. 1.

$$K = \frac{\Delta P_t}{\frac{1}{2} \rho u^2} \quad \text{Eqn. 1}$$

A sensitivity study was conducted, varying the K-loss coefficient attributed to grommet wakes from 0.1 to 0.4, and the liner pressure profile variation was inconsequential.

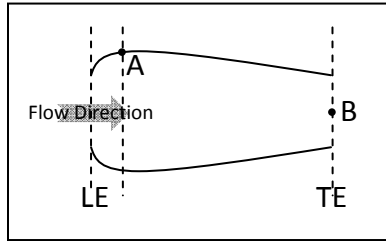


Figure 1

The coolant temperature increases significantly along the axial direction of the can. A typical, circumferentially uniform, linear trend was employed, using engine T_3 input to dial in accuracy. P_3 is the pressure at the station at the inlet to the pre-diffuser. P_{31} is the pressure at the combustor inlets. P_{31} was also available from measured engine data. Though the results were generated for various power settings in Table 2, only those results for full power setting are presented because the liner pressure profiles ($\%P_{31}$) were virtually the same. Referring to Fig. 1, static pressure ports on the inner surface of the liner at A typically measure a pressure near to the exit total pressure at B; therefore, the total pressure, P_4 , is assumed to be the static pressure $P_{s,31}$. Flow through the cooling exit holes is driven by the upstream static pressure. The pressure drop is assumed to be the difference between the static pressure inside the liner at that location and P_4 .

Table 2. Instrumentation data used for FABL calculation

Power Setting	P_{31} (psia)	P_4 (psia)	T_{31} ($^{\circ}$ F)
100%	275.5	270.1	879.9
75%	242.8	238.0	819.0
50%	197.8	194.0	742.9

The K-loss coefficient through the liner exit is modeled as a sudden expansion using Eqn. 2, where AR is the ratio between the combustor exit area and the liner exit area.

$$\frac{P_{t_1} - P_{t_2}}{\frac{1}{2} \rho u^2} = \left(1 - \frac{1}{AR}\right)^2 = K \quad \text{Eqn. 2}$$

Phase I design calculation

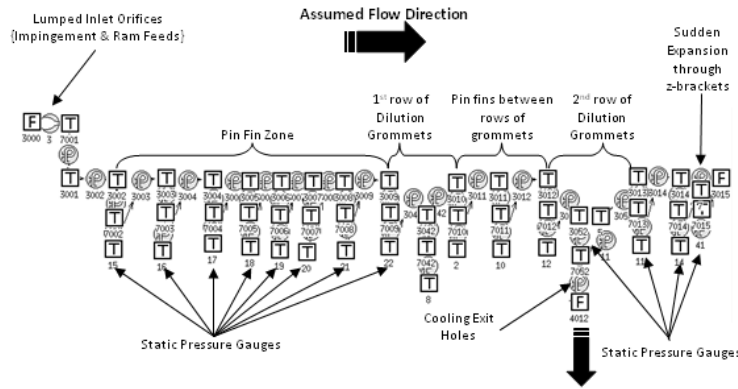


Figure 2. Flow Network Diagram

The hot flow results presented in Fig. 3 were generated using pressure and temperature boundary conditions available from test data for the phase I design with the annular cold flow gap height decreased by predicted radial expansion of the liner. A typical standard outflow margin is 1% of the source pressure to prevent backflow.

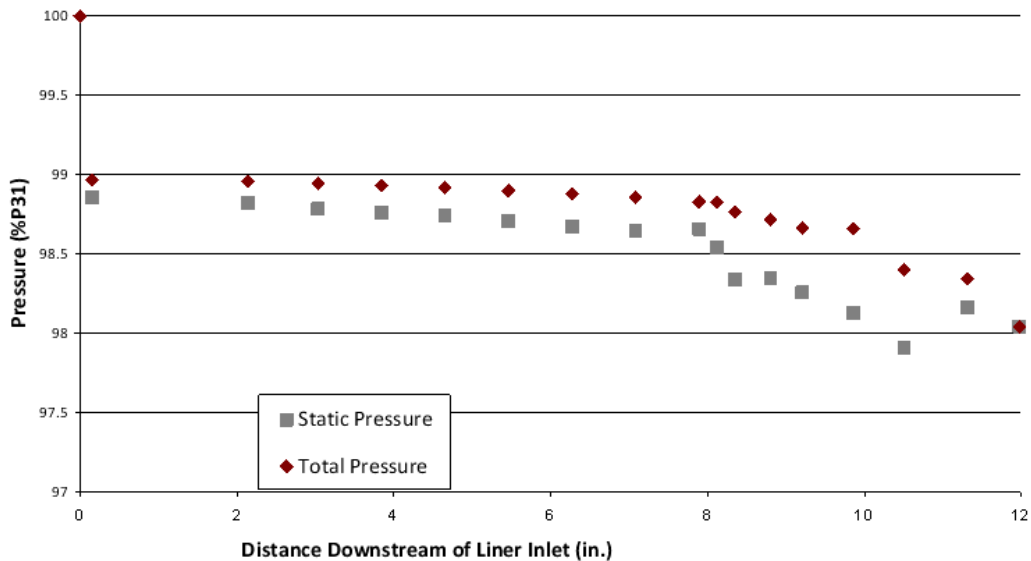


Figure 3. Hot flow total and static pressure profiles

Fig. 4 is a comparison of the total pressure loss attributed to each of the modeled features between hot and cold flow inputs (as a percent of the overall pressure loss). The losses

through the inlets are higher for the hot flow since the annular inlet flow area is decreased.

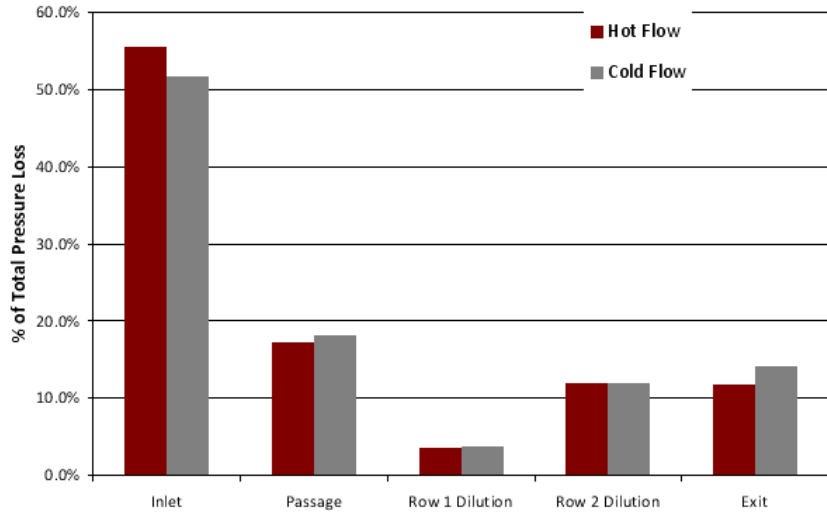


Figure 4. Hot vs. Cold total pressure loss comparison

Phase II design prediction

For the phase I engine test, one of the cans tested had additional impingement cooling holes to aid in cooling hot spots where the fluid velocities are low. Thermal paint contours and temperature crystal measurements on the can indicate that the cooling holes were effective. The secondary flow model was altered to include this revision. Fig. 11 is the secondary flow prediction for the revised design at the target overall pressure drop.

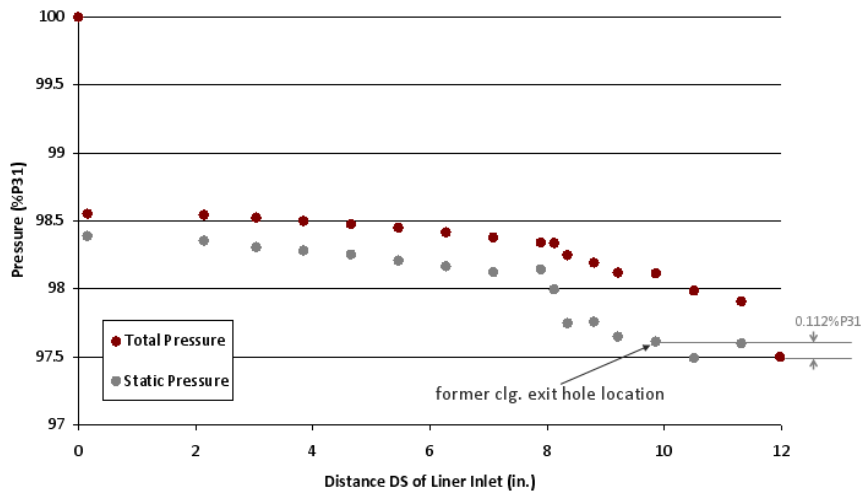


Figure 5. Liner pressure profile: hot flow, target $dP/P = 2.5\%$, cooling exit holes closed, additional impingement cooling

Segmented annulus model for Combustor 1

Since the liner is not symmetric, an attempt was made to model the circumferential variation of the liner. While constructing a reliable full annulus model,

described above, the sequence of resistors and chambers was modified, replicated, and conjoined in an attempt to represent control volumes that form annular sectors. The pull planes, barren real estate on the liner surface where a manufacturing tool required that there be no obstruction, defined the edges of the sectors. Communication lines were added to recover some of the 3-dimensionality. The motivation for this effort was to better resolve the circumferential variation and predict hot gas ingestion into the liner in the sector where metal distress was typically most extreme. Ultimately, the effort was abandoned because of questionable fidelity and because the full-annular model was sufficient in aiding the root cause analysis.

Introduction to DLN

A turbine with a conventional diffusion combustor which injects diluents to suppress NO_x will use an underlying algorithm to control steam or water injection; however, these methods are limited in their ability to reach extremely low emissions levels required in many localities where using de-ionized water may not be cost effective.

Research and design has shown that a decrease in NO_x emissions is possible during combustion of lean homogeneous mixtures of natural gas and air. Design of a successful Dry-Low- NO_x (DLN) combustor for a heavy-duty gas turbine requires the designers to develop hardware features and operational methods that simultaneously allow the equivalence ratio and residence time in the flame zone to be low enough to achieve low NO_x , but with acceptable levels of combustion noise (dynamics), stability throughout the load range and sufficient residence time for CO burnout.

The introduction of this method of combustion by almost all the leading gas-turbine companies resulted in nitrogen oxide concentrations <25 ppm. The majority of combustors are designed with two (or more) independently controlled stages of fuel admission during the start-up and loading of the gas turbine. Typically, the dilution zone (the region of the combustor immediately downstream from the flame zone) provides a region for CO burnout and for shaping the gas temperature profile exiting the combustion system. Instead of producing a temporally uniform air-fuel ratio, the premixer produces a uniform spatially mixed air-fuel ratio, which may vary cyclically in time at the pressure fluctuation frequency. As heat-release from the combustion process is closely related to air-fuel ratio, temporal variations within the premixer produce temporal variations in heat-release within the combustion chamber. These in turn generate the pressure fluctuations within the combustion chamber that cause the air-fuel ratio within the mixing duct to oscillate on the next cycle. Thus the feedback loop is established.

DLN/DLE Competitor Assessment

The objective of compiling and scaling the parameters of available Dry-Low- NO_x /Dry-Low-Emission (DLN/DLE) combustion systems in the same family as the concept combustor was to provide design-space boundaries and develop an idea of how aggressive the design can be for the subsequent design iteration. The conclusion is that the previous iteration of the combustor design is oversized. Using published information, and several available geometries, competitor designs were surveyed and results compiled for comparison. This information includes length : diameter ratio, combustor volume, residence time, reference velocity, dump ratio, volumetric flow rate, combustor surface

area, and combustor air loading parameter. Aspects of the methodology are included in the Appendix.

Combustor 2 Secondary Flow Model

After learning how to use the secondary flow code, the lessons learned were applied to model the flow through a single axially staged combustor concept. The concept combustor model *includes* the flow through the combustion zone and transition duct. The modeled features are the impingement cooling sleeve airflow, the flow sleeve, the cap and liner assembly, premixer, combustion zone, secondary airflow, transition piece, and interface leakage.

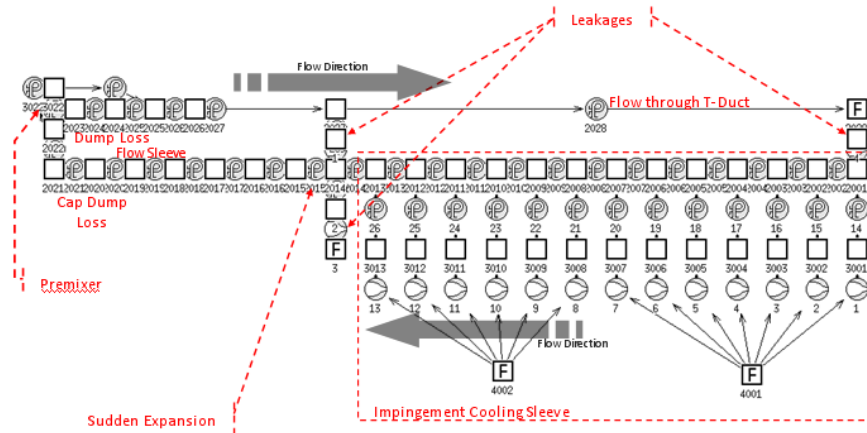


Figure 6. Concept combustor flow network

Calculating the cross-sectional area of the transition piece is not straightforward. From the primary combustion stage exit, where the cross-section is circular, to the 1st stage HPT vane, where the cross-section is an annular sector, an area function of a congruent, but smaller, piece was provided. The area function was scaled by the ratio of the baseline concept combustor can primary stage exit area to the smaller circular cross-section area. The scaled area function was used to compute the flow area inside the transition duct, and in the impingement flow sleeve.

For lack of pressure distribution information about the impingement cooling sleeve, the source pressure for all rows of impingement cooling holes is assumed to be the same. The simplification implemented in the concept combustor model may be accurate compared with cold flow measurements since the source pressure is atmospheric everywhere. No impingement cooling inlet hole dimensions were prescribed, so the modeled impingement cooling sleeve consists of 13 rings of cooling holes. Four hole sizes were used, but each ring is comprised of only one size impingement cooling hole for simplicity. The hole diameter is chosen to maintain approximately equivalent edge-to-edge spacing between holes around each ring.

The dump loss from the annular flow area into the front end plenum cross-section area is used to compute the K-loss coefficient via Eqn. 2, and similarly for the dump loss from the premixer exit area to the primary combustion zone flow area.

Leakage flow areas are added at the T-duct/flow sleeve and at the T-duct/HPT interfaces.

Appendix: Competition Scaling Methodology

- For known OPR, and unknown T3, compressor efficiency was either pulled from available estimated or assumed

- This method was verified by available data

- $\frac{T_{03}}{T_{02}} = OPR^{(\gamma-1)/\eta_{compress}}$ $90\% \leq \eta_{compress} \leq 95\%$

- For unknown W31

- This method was verified by available data which matched the estimate to within $\pm 10\%$ of the correct value

- All values of mass flow presented herein were derived using this method

- $\dot{m} = \frac{P}{c_p \cdot dT}$ $\eta_{TH} = \frac{P_{shaft}}{\dot{m}_f Q_R}$

- For axially staged combustors, the momentum flux through both primary and secondary zones assumed equal

- ...The mass flow split to stage 1 inversely proportional to the dump ratio from the primary to secondary zone

- This method was not verified

- $\dot{m}_{stage\ 1} \propto \left(\frac{A_2}{A_1}\right)^{-1} W_{31}$